Arabian Journal of Chemistry (2012) **5**, 213–218

King Saud University

Arabian Journal of Chemistry

www.ksu.edu.sa
www.sciencedirect.com

ORIGINAL ARTICLE

On the corrosion inhibition of iron in hydrochloric acid solutions, Part I: Electrochemical DC and AC studies

K.F. Khaled [a,b,*], S.S. Abdel-Rehim [c], G.B. Sakr [d]

[a] *Electrochemistry Research Laboratory, Ain Shams University, Faculty of Education, Chemistry Department, Roxy, Cairo, Egypt*
[b] *Materials and Corrosion Laboratory, Taif University, Faculty of Science, Chemistry Department, Taif, Hawiya 888, Saudi Arabia*
[c] *Ain Shams University, Faculty of Science, Chemistry Department, Abbassia, Cairo, Egypt*
[d] *Ain Shams University, Faculty of Education, Physics Department, Roxy, Cairo, Egypt*

Received 28 June 2010; accepted 30 August 2010
Available online 7 September 2010

KEYWORDS

Iron;
Acid inhibition;
Polarization;
EIS

Abstract The inhibitive action of 4-methyl pyrazole (4MP) against the corrosion of iron (99.9999%) in solutions of hydrochloric acid has been studied using potentiodynamic polarization and electrochemical impedance spectroscopy (EIS). At inhibitor concentration range (10^{-3}–10^{-2} M) in 1.0 M acid, the results showed that 4MP suppressed mainly the anodic processes of iron corrosion in 1.0 M HCl by adsorption on the iron surface according to Temkin adsorption isotherm. Both potentiodynamic and EIS measurements reveal that 4MP inhibits the iron corrosion in 1.0 M HCl and that the efficiency increases with increasing inhibitor concentration. Data obtained from EIS were analyzed to model the corrosion inhibition process through an equivalent circuit.

1. Introduction

Acid solutions are generally used for the pickling, industrial acid cleaning, acid descaling and oil well acidizing, etc (Zhang and Hua, 2009; Machnikova et al., 2008; Li et al., 2007; Khaled and Hackerman, 2005). Iron and its alloys which are widely used in a lot of industrial processes could corrode during these acidic applications particularly with the use of hydrochloric and sulphuric acid. The corrosion prevention of metals has always been an important subject to be dealt with. The decreasing corrosion rate of metals provides savings of resources and economical benefits during the industrial applications. The prevention of corrosion is vital not only for increasing the lifetime of equipments but also for decreasing the dissolution of toxic metals from the components into the environment. The use of organic molecules as corrosion inhibitors is one of the most practical methods for protecting

* Corresponding author at: Electrochemistry Research Laboratory, Ain Shams University, Faculty of Education, Chemistry Department, Roxy, Cairo, Egypt. Tel.: +966 550670425.
E-mail address: khaledrice2003@yahoo.com (K.F. Khaled).

Peer review under responsibility of King Saud University.
doi:10.1016/j.arabjc.2010.08.015

Production and hosting by Elsevier

metals against corrosion and it is becoming increasingly popular. In recent years, a considerable amount of effort is devoted to find novel, economical and efficient corrosion inhibitors. Organic compounds bearing heteroatoms with high electron density such as phosphor, sulphur, nitrogen, oxygen or those containing multiple bonds which are considered as adsorption centers, are effective as corrosion inhibitors (Quraishi and Rawat, 2002; Abd El Maksoud, 2002; Abdallah, 2002). The compounds which contain both nitrogen and sulphur in their molecular structure have exhibited greater inhibition compared with those which contain only one of these atoms (Hassan et al., 2007; Abdoud et al., 2007; Khaled, 2010).

In continuation of the work on the development of corrosion inhibitors for acidic solutions (Khaled et al., 2009, 2010; Khaled and Amin, 2009a,b; Khaled, 2009), the authors have studied the corrosion-inhibiting behavior of 4-methy pyrazole (4MP), against the corrosion of iron (99.9999%) in solutions of hydrochloric acid. The aim of this work is devoted to the study the inhibition characteristics of (4MP) for acid corrosion of iron 99.9999 by electrochemical measurements which include both dc polarization and ac impedance measurements.

2. Experimental details

Iron specimens from Johnson Mattey (Puratronic, 99.9999%) were mounted in Teflon with surface area (0.28 cm^2). An epoxy resin was used to fill the space between the Teflon and the iron electrode in order to prevent crevice corrosion. The electrochemical measurements were performed in a typical three-compartment glass cell; the iron specimen was the working electrode, Pt gauze was used as an auxiliary electrode and a saturated calomel electrode(SCE) was used as a reference electrode. The auxiliary electrode was separated from the working electrode compartment by fritted glass. The reference electrode was connected to the Luggin capillary to minimize IR drop and chloride contamination.

Solutions were prepared from deionized water of the resistivity which equals 13 MΩ cm, The specimens were polished with emery papers, washed with bi-distilled water, etched in 12 M HCl for 10 min, and rinsed with redistilled water and then with acetone before immersion into the solutions. This procedure was used to ensure a reproducible starting surface state. The electrode potential was allowed to stabilize 30 min before starting the measurements. All the experiments were conducted at 25 °C. The solutions were prepared by mixing HCl (Fisher Scientific) with 4-methyl pyrazole (4MP) from Aldrich, were dissolved in HCl without any pretreatment. The measurements were performed by means of EG&G Princeton Applied Research Potentiosate/Galvanostat (PAR model 273) in combination with a Solarton 1250 frequency response analyzer were used for polarization and capacitance measurements. The system is attached to a PC for collecting data. The potentiodynamic current–potential curves were recorded by changing the electrode potential automatically from −1000 to 0.000 mV_{SCE} with a scan rate of 1.0 mVs^{-1}. Electrochemical impedance spectroscopy (EIS) measurements were carried out in a frequency range of 10 KHz–0.0001 Hz using an amplitude of 5 mV peak to peak using ac signal at open circuit potential. The softwares used in this study are electrochemical impedance software (Model 398), corrosion software (Model 352-252, Version 2.23) and equivalent circuit software (EQUIVCRT.PAS).

3. Results and discussion

3.1. Potentiodynamic polarization measurements

Some corrosion phenomena can be explained in terms of electrochemical reactions. It follows then, that electrochemical techniques can be used to study these phenomena. Measurements of current–potential values under carefully controlled conditions can yield information on corrosion rates, coatings and films, passivity, pitting tendencies and other important phenomena. Potentiodynamic anodic polarization is the characterization of a metal specimen by its current–potential relationship. The specimen potential is scanned in the positive – going direction. These measurements are used to determine corrosion characteristics of a metal specimen in aqueous environments. A complete current–potential plot of a specimen can be measured in a few hours or in some cases in a few minutes (Basics of corrosion measurements, 1982).

When an iron specimen is immersed in a corrosive medium (HCl in this case), both reduction and oxidation processes occur on its surface. Typically the iron specimen oxidizes (corrodes) and the medium (HCl in this case) is reduced. This means that the hydrogen ions are reduced. The iron specimen can function as both anode and cathode, and both anodic and cathodic currents occur on the specimen surface. Any corrosion processes that occur are usually a result of anodic currents. When an iron specimen is in contact with a corrosive liquid and the specimen is not connected to any instrumentation – as it would be "in service" – the specimen assumes a potential (relative to a reference electrode) termed as the corrosion potential, E_{corr}. A specimen at E_{corr} has both anodic and cathodic currents present on its surface. However, these currents are exactly equal in magnitude so there is no net current to be measured. The specimen is at equilibrium with the environment (even though it may be visibly corroding). E_{corr} can be defined as the potential at which the rate of oxidation is exactly equal to the rate of reduction. Experimentally one measures polarization characteristics by plotting the external current response as a function of the applied potential. Since the measured current can vary over several orders of magni-

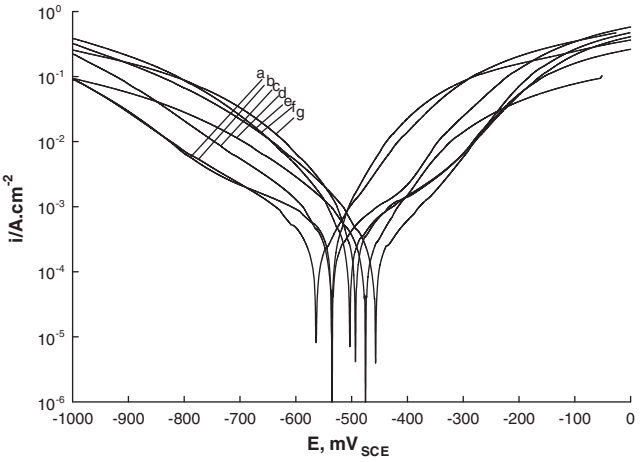

Figure 1 Potentiodynamic polarization curves of iron immersed in 1.0 M HCl and different concentrations of 4-methyl pyrazole (4MP): (a) Blank, (b) 1×10^{-3} , (c) $3 \times 10{-}3$, (d) 5×10^{-3} , (e) 7×10^{-3} , (f) 9×10^{-3} , (g) 10×10^{-3}.

tude, usually the log current function is plotted vs. potential on a semi-log chart. This plot is termed as a potentiodynamic polarization plot. In this study we will use Tafel plot to describe the polarization characteristics of the corrosion system. The corrosion current density, i_{corr}, is obtained from Tafel plot by extrapolating the linear portion of the curve to E_{corr}, as shown in Fig. 1. The corrosion rate can be calculated from the corrosion current by using Eq. (1), Basics of corrosion measurements, 1982.

$$\text{Corrosion rate(mpy)} = \frac{0.13 i_{corr}(\text{E.W.})}{d} \quad (1)$$

where i_{corr} = corrosion current density, μA/cm^2, E.W. = equivalent weight of iron specimen, g, d = density of the corroding species, g/cm^3

Tafel plots can provide a direct measure of the corrosion current, which can be related to the corrosion rate. Tafel plots for the iron specimen immersed in 1.0 M HCl in the absence and in the presence of different concentrations of 4-methyl pyrazole is presented in Fig. 1.

Fig. 1 shows that the addition of (4MP) to the acid solution shifts the anodic polarization to more positive and the cathodic polarization to more negative values. The effect of (4MP) is more pronounced on anodic polarization than on cathodic polarization. Values of the electrochemical parameters and the percentage inhibition efficiency δ% are given in Table 1. The inhibition efficiency calculated from potentiodynamic polarization measurements, δ% is given from the Eq. (2) Abd El-Rehim et al., 1999:

$$\delta\% = \left(1 - \frac{i_{corr}}{i^{o}_{corr}}\right) \times 100 \quad (2)$$

where i^{o}_{corr} and i_{corr} are the uninhibited and inhibited corrosion current densities, respectively, determined by extrapolation of Tafel lines. The values of i_{corr} decrease with increasing concentration, the decrease in i_{corr} is associated with a shift in E_{corr} to less negative values. These results suggest that (4MP) behaves mainly as an anodic inhibitor. The approximately constant values of the Tafel slopes (near 0.09 V dec^{-1} for b_a and 0.13 V dec^{-1} for b_c suggest that the inhibition mechanism for (4MP) involves a single reaction site blocking (Moretti et al., 1996; Hoar and Khera, 1960).

By Analysis of Fig. 1, we can determine different corrosion kinetic parameters for iron in 1.0 M HCl in the absence and presence of different concentrations of (4MP). These kinetic parameters are reported in Table 1.

It is seen from Table 1 that the addition of (4MP) reduces the values of i_{corr} to an extent, which increases with increasing concentration. This indicates that (4MP) inhibit the corrosion of iron in HCl solutions. Inspection of Table 1 shows that the maximum inhibition (lowest corrosion current density) is achieved at the highest concentration. It can also be seen that increasing concentrations of (4MP) shift the corrosion potential E_{corr} to less negative values, thereby showing that (4MP) is adsorbed on the iron surface and this kind of inhibitor behaves mainly as anodic-type inhibitors. The anodic and cathodic Tafel constants (b_a and b_c) do not change significantly with increasing concentration of the inhibitor, i.e. (4MP) affects both the anodic and cathodic overpotentials and shifts Tafel lines parallely in both directions. This indicates that this inhibitor at varying concentrations do not alter the reaction mechanism. This suggests that the inhibiting action of such compounds occurs by simple site blocking of the electrode, thus decreasing the surface area available for corrosion reactions (Khaled, 2003). The values of Tafel slops (b_a and b_c) are in good agreement with the values reported previously for iron in 1.0 M HCl (Grauer et al., 1982). Table 1 also shows that by increasing (4MP) concentration inhibition efficiency increases and corrosion rate decreases.

Fig. 2 shows the effect of (4MP) on the corrosion rate of iron in 1.0 M HCl at 25 °C. The corrosion rate decreases with an increase in the concentration of (4MP), presumably because of adsorption on the iron surface. Fig. 2 also shows that the inhibition efficiency δ% increases with increasing concentration of (4MP).

Sieverts and Lueg firstly and systematically investigated the dependence of the corrosion rate of iron in acids upon the concentration of the organic inhibitors (Sieverts and Lueg, 1923). They established that at constant temperatures the curves representing this relationship (Fig. 2) have the form of adsorption isotherms if the concentration of the inhibitor is plotted

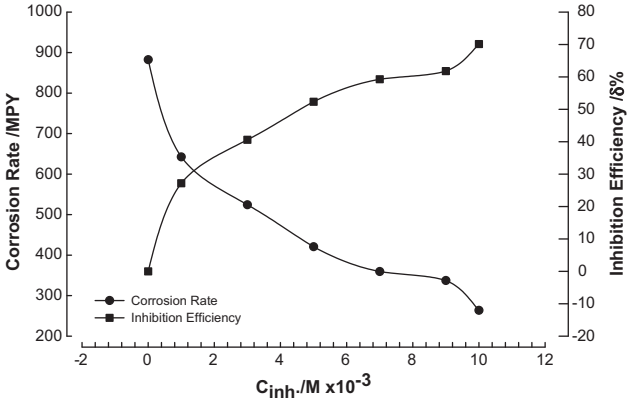

Figure 2 The corrosion rate/mpy and the inhibition efficiency δ% for iron in 1.0 M HCl containing different concentrations of 4-methyl pyrazole (MPA) (from potentiodynamic data).

Table 1 Electrochemical parameters for iron in 1.0 M HCl with different concentrations of 4-methyl pyrazole at 25 °C.

Conc. (M)	I_{corr} (μA cm^{-2})	$-E_{corr}$ (V)	$-b_c$ (V dec^{-1})	$-b_a$ (V dec^{-1})	C.R (mpy)	δ%
Blank	965.2	0.535	0.130	0.091	882.5	–
1×10^{-3}	702.7	0.513	0.122	0.099	642.5	27.19
3×10^{-3}	573.3	0.498	0.119	0.083	524.2	40.60
5×10^{-3}	460.0	0.499	0.132	0.105	420.6	52.34
7×10^{-3}	393.2	0.487	0.145	0.100	359.5	59.26
9×10^{-3}	368.8	0.475	0.138	0.107	337.2	61.79
10×10^{-3}	288.3	0.450	0.122	0.109	263.6	70.13

on the horizontal axis and the values of the inhibition efficiency on the vertical axis. If, on the other hand, the rates of corrosion are plotted as ordinates, the curves assume the form of adsorptions turned through 180°. This led Sieverts and Lueg to suggest an adsorption mechanism for the action of organic corrosion inhibitors in acids, and many latter works have supported this hypothesis (Putilova et al., 1960).

3.2. Electrochemical impedance spectroscopy

The popularity of the EIS technique for studying corroding systems is growing. EIS technique uses the rapid relaxation phenomena, which can be varied over a wide range of frequency. Impedance is determined by applying an ac voltage at a specific frequency and measuring the associated current. From the voltage and the current, impedance can be calculated for that frequency. By means of EIS technique a spectrum of impedance of the system under a series of frequencies can be observed.

Fig. 3 shows the Nyquist plots of iron in 1.0 M HCl without and with various concentrations of 4MP (10^{-3}–10^{-2} M) at 25 °C. The impedance diagrams obtained are not perfect semicircles and this difference has been attributed to frequency dispersion (Mansfeld et al., 1982). The charge transfer resistance R_{ct} is calculated from the difference in impedance at lower and higher frequencies, as suggested by Harnyama and Tsuru (Tsuru et al., 1978). To obtain the double layer capacitance C_{dl}, the frequency at which the imaginary component of the impedance is maximum ($-Z''_{img}$), is found and C_{dl} values are obtained from the Eq. (3) Ross Macdonald, 1987.

$$F(-Z'_{max}) = \frac{1}{2\pi C_{dl} R_{ct}} \quad (3)$$

From the charge transfer resistance we can calculate the inhibition efficiency of the corrosion of iron, as in Eq. (4) Abd El-Rehim et al., 1999.

$$\phi\% = \left(1 - \frac{R_{ct}^{o}}{R_{ct}}\right) \times 100 \quad (4)$$

where R_{ct}^{o} and R_{ct} are the charge transfer resistance values without and with the inhibitor, respectively. The impedance parameters derived from this investigation are given in Table 2. Fig. 4 shows that by increasing the concentration of 4MP, corrosion rate ($1/R_{ct}$) decreases and the inhibition efficiency calculated from EIS measurements φ% increases. The equivalent circuit model used to fit the experimental results is suggested in Fig. 5, the suggested model is used to generate a simulated data, which is fitted well with experimental data as shown in the examples Fig. 6 (a,b,c and d). The charge transfer resistance R_{ct} and the double layer capacitance were calculated and given in Table 2. The fitted parameters were calculated using equivalent circuit in Fig. 5 is presented in Table 3. It is clear that by increasing the concentration of the inhibitor (4MP) the corrosion rate $1/R_{ct}$ is decreased and at the same time the inhibition efficiency φ% increases.

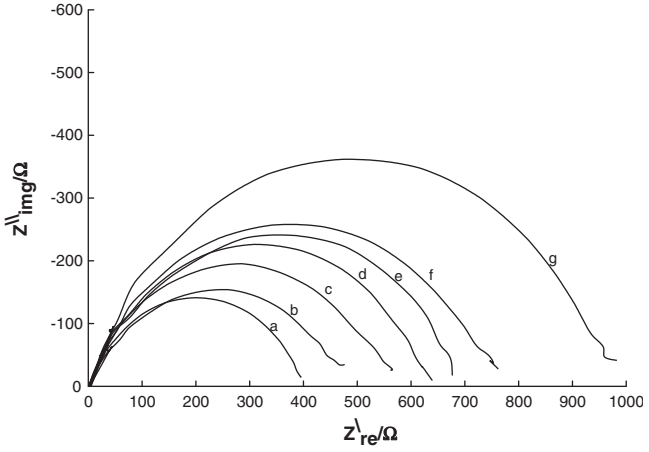

Figure 3 Complex-plane impedance of iron in 1.0 M HCl in the presence of different concentrations of 4-methyl pyrazole (4MP) at 25 °C, (a) Blank, (b) 1×10^{-3} M, (c) 3×10^{-3} M, (d) 5×10^{-3} M, (e) 7×10^{-3} M, (f) 9×10^{-3} M, (g) 10×10^{-3} M.

Table 2 Impedance data of iron in 1.0 M HCl solution containing different concentrations of 4-methyl pyrazole at 25 °C.

Conc. (M)	R_{ct} (Ohm cm^2)	$1/R_{ct}$	C_{dl} (μF cm^{-2})	φ%
Blank	427.4	2.34E-3	93.5	–
1×10^{-3}	535.66	1.86E-3	74.6	20.21
3×10^{-3}	622.49	1.61E-3	64.2	31.34
5×10^{-3}	679.71	1.47E-3	58.8	37.12
7×10^{-3}	752.8	1.33E-3	53.1	43.22
9×10^{-3}	811.16	1.23E-3	49.3	47.31
10×10^{-3}	998.13	1.00E-3	40.1	57.18

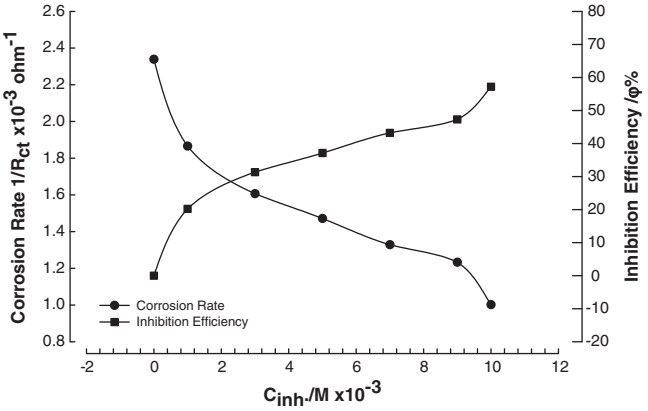

Figure 4 The inverse charge transfer resistance $1/R$ct and the inhibition efficiency φ% for iron in 1.0 M HCl containing different concentrations of 4-methyl pyrazole (4MP) (from impedance data).

Fig. 5 shows the equivalent circuit used to fitting the experimental impedance data which is described in detail elsewhere (Abd El-Rehim et al., 1999). Often a CPE is used in a model in place of a capacitor C_{dl} (double layer capacity) to compensate for non-homogeneity in the system (Abd El-Rehim et al.,

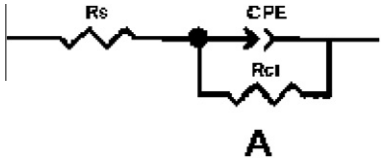

Figure 5 Equivalent circuit model for iron/1.0 M HCl interface.

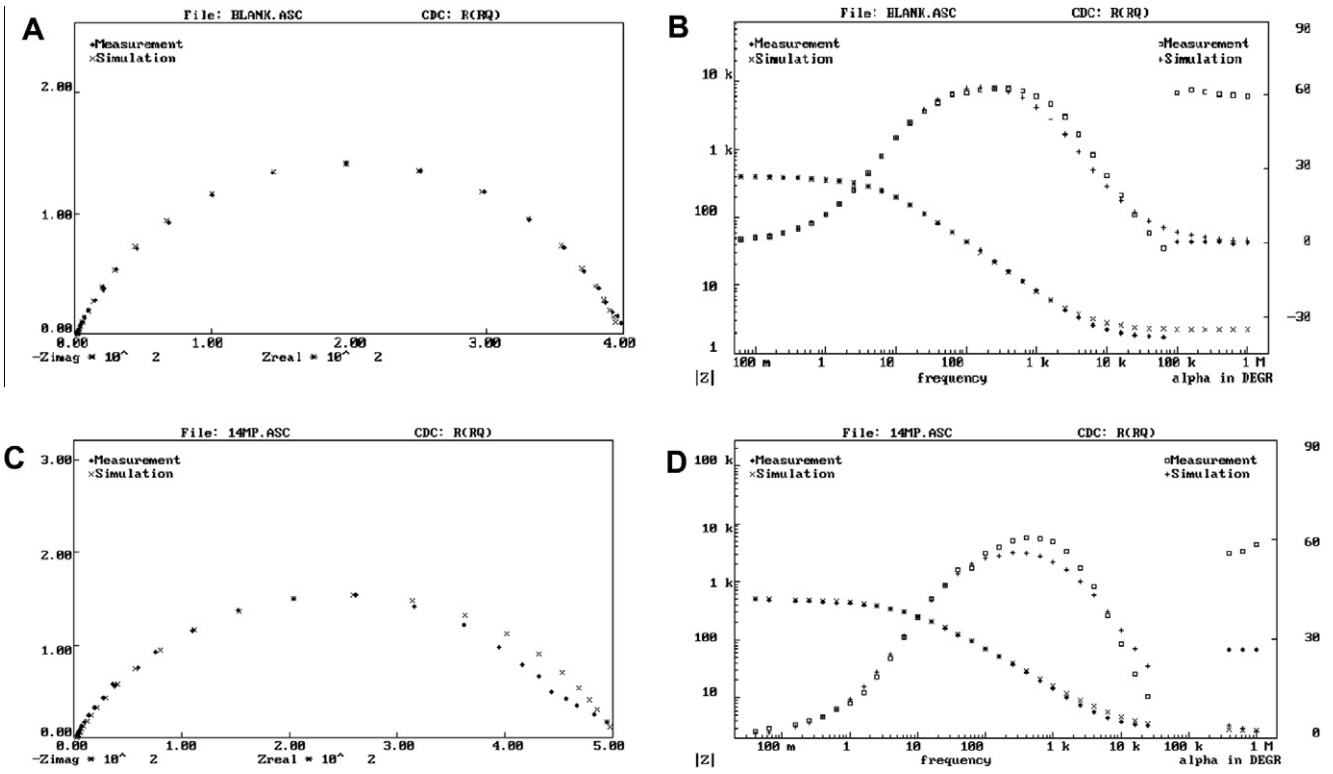

Figure 6 Impedance data for corroding iron at corrosion potential in 1.0 M HCl at 25 °C. Plot (A, C) shows the complex plan representation each data point corresponds to a different frequency; Plot (B, D) shows the magnitude and phase angel of the impedance as a function of frequency. Plot (A, B) for blank, and (C, D) for 10^{-3} M 4-methyl pyrazole (4MP)/1.0 M HCl. (+) curves are the nonlinear regreation to the data, open symbols are experimental data.

1999). For example a rough or porous surface can cause a double layer capacitance to appear as a CPE with an n value between 0.9 and 1.

Excellent fit with this model was obtained with our experimental data (Fig. 6). It is observed that the fitted data match the experimental data, with an acceptable error.

In order to understand the mechanism of corrosion inhibitor, the adsorption behavior of the organic adsorbate (4MP) on the iron surface must be known (Al-Andis et al., 1995). The degree of surface coverage (θ) for different concentrations of (4MP) in 1.0 M HCl has been evaluated from EIS measurements using Eq. (5) Abd El-Rehim et al., 1999.

$$\theta = \left(1 - \frac{R_{ct}^{o}}{R_{ct}}\right) \tag{5}$$

The data were tested graphically by fitting to various isotherms. A straight line was obtained on plotting θ vs. log C (Fig. 7) suggesting that the adsorption of (4MP) from 1.0 M HCl on an iron surface follow Temkin's adsorption isotherm.

The Temkin isotherm characterizes the adsorption of uncharged molecules on a heterogeneous surface, where θ is a linear function of ln$C$ (Morad and Kamal El-Dean, 2006)

$$\theta = (1/f)\mathrm{In}(K_{ads}C) \tag{6}$$

f is a factor of energetic inhomogeneity in the surface, C is the adsorbate concentration, and K_{ads} is the equilibrium constant for the adsorption process, which is related to the standard free energy of adsorption (ΔG_{ads}^{o}) by

$$K_{ads} = \frac{1}{55.5}\exp\left(-\frac{\Delta G_{ads}^{o}}{RT}\right) \tag{7}$$

The linear plot of θ vs. ln$C$ as shown in Fig. 7 is in agreement with the Temkin equation. The calculated values of the adsorption parameters f, lnK_{ads}, and ΔG_{ads}^{o} are 0.5, and -11.2 kJmol^{-1}, respectively. The negative value of ΔG_{ads}^{o} implies that the adsorption of 4MP on the iron surface is allowed from the thermodynamics point of view and indicates that the inhibitor is weakly adsorbed. Values of K_{ads} and ΔG_{ads}^{o} were found to be 1.665 M^{-1} to -11.2 kJ mol^{-1}, respectively.

The adsorption of 4MP on the metal surface can occur either directly on the basis of donor-acceptor interactions between the π-electrons of the heterocyclic compound and the vacant d-orbitals of iron surface atoms. Or the interaction of MPA with already adsorbed chloride (Hackerman et al., 1966). The performance of 4-methylpyrazole as an inhibitor in 1.0 M HCl can be explained in the following way. In aqueous acidic solutions, the 4-methylpyrazole compound exists either as neutral molecules or in the form of cations. Amines may be adsorbed on the metal surface in the form of neutral molecules, involving the displacement of water molecules from the metal surface and sharing of electrons between the nitrogen atoms and the metal surface (Khaled et al., 2009). Amines and heterocyclic nitrogen compounds may also adsorb trough electrostatic interactions between the positively charged nitrogen

Table 3 Circuit element R_s, R_p, and CPE values and their error percent for iron in 1.0 M HCl in the absence and presence of 4-methyl pyrazole using equivalent circuit in Fig. 5.

4-methyl pyrazole	Element	Value	Error	Error %
Blank	R_S	1.6	0.05	3.1
	CPE	1.4E-4	6.5E-6	4.71
	n	0.78	6.3E-3	0.79
	R_{ct}	395.8	7.22	1.83
0.001 M	R_S	2.6	0.132	4.8
	CPE	0.0001	8.5E-6	8.1
	n	0.76	0.02	1.4
	R_{ct}	472.7	14.8	3.13
0.003 M	R_S	3.2	0.15	4.5
	CPE	5.4E-5	1.6E-5	30.14
	n	0.08	0.03	3.9
	R_{ct}	601.4	14.65	2.4
0.005 M	R_S	3.43	0.11	3.2
	CPE	7.8E-5	5.5E-6	7.02
	n	0.82	0.01	1.2
	R_{ct}	619.2	15.5	2.51
0.007 M	R_S	3.03	0.1	3.2
	CPE	9.2E-5	4.6E-6	5.1
	n	0.78	0.01	0.8
	R_{ct}	675.3	11.72	1.17
0.009 M	R_S	1.451	0.12	7.45
	CPE	8.51E-5	3.39E-6	3.9
	n	0.78	0.005	0.69
	R_{ct}	748.5	10.31	1.37
0.01 M	R_S	4.7	0.09	1.9
	CPE	5.5E-5	1.6E-4	3.1
	n	0.82	0.004	0.52
	R_{ct}	878.9	9.6	1.1

atom and the negatively charged metal surface (Khaled et al., 2009). The presence of lone pairs and π-electrons of the 4-methypyrazole compound enhanced the inhibitory effect of this compound.

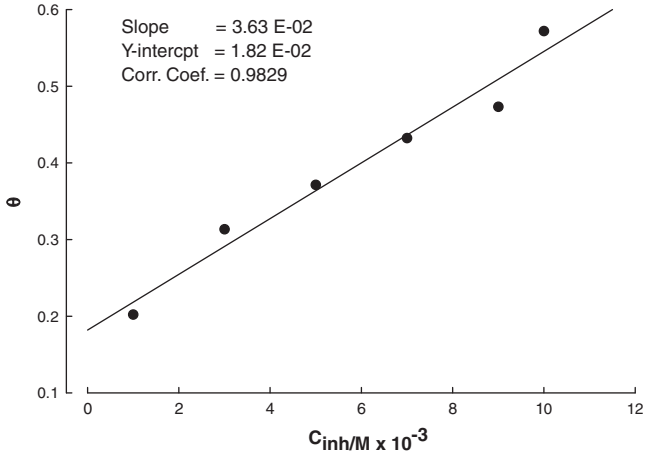

Figure 7 Temkin adsorption plots for iron in 1.0 M HCl containing different concentrations of 4-methyl pyrazole.

4. Conclusion

4-Methyl pyrazole has shown inhibiting properties for iron corrosion in 1.0 M HCl. 4MP is anodic-type inhibitor. Both potentiodynamic and EIS measurements reveal that 4MP inhibits the iron corrosion in 1.0 M HCl and that the efficiency increases with increasing inhibitor concentration. 4MP acts as a corrosion inhibitor by adsorption on the iron surface according to Temkin adsorption isotherm.

References

Abd El Maksoud, S.A., 2002. Corros. Sci. 44, 803–813.
Abd El-Rehim, S.S., Ibrahim, Magdy A.M., Khaled, K.F., 1999. J. Appl. Electrochem. 29, 593–599.
Abdallah, M., 2002. Corros. Sci. 44, 717–728.
Abdoud, Y., Abourrriche, A., Saffaj, T., Berrada, M., Charrouf, M., Bennamara, A., Al Himidi, N., Al Himidi, H., Hannache, H., 2007. Mater. Chem. Phys. 105, 1–5.
Al-Andis, N., Khamis, B., AI-Mayouf, A., Aboul-Enein, H., 1995. Corros. Prev. Control 424, 13.
Grauer, R., Moreland, P.J., Pini, G., 1982. Presented in The European Federation of Corrosion (ed.), A working Party Report on Physicochemical Teasting Methods of Corrosion-Fundamental and Application. European Federation of Corrosion, NACE.
Hackerman, N., Snavely Jr., E., Payne Jr., J.S., 1966. Electrochem. Soc. 113, 677.
Hassan, H.H., Adbelghani, E., Amin, M.A., 2007. Electrochim. Acta 52, 6359–6366.
Hoar, T.P., Khera, R.P., 1960. In: Proc. Ist European Symposium on Corrosion Inhibitors, vol. 73. University of Ferrara, Ferrara, Italy.
Khaled, K.F., 2003. Electrochim. Acta 48, 2493–2503.
Khaled, K.F., 2009. J. Solid State Electrochem. 13, 1743.
Khaled, K.F., 2010. J. Electrochem. Soc. 157, C116–C124.
Khaled, K.F., Amin, Mohamed A., 2009a. J. Appl. Electrochem. 39, 2553.
Khaled, K.F., Amin, Mohamed A., 2009b. Corros. Sci. 51, 1964.
Khaled, K.F., Hackerman, N., 2005. Appl. Surf. Sci. 240, 327–340.
Khaled, K.F., Fadlallah, S., Hammouti, B., 2009. Mater. Chem. Phys. 117, 155.
Khaled, K.F., Amin, Mohamed A., Almobarak, N.A., 2010. J. Appl. Electrochem. 39, 601–613.
Li, W., He, Q., Pei, C., Hou, B., 2007. Electrochim. Acta 52, 6386–6394.
Machnikova, E., Whitmire, K.H., Hackerman, N., 2008. Electrochim. Acta 53, 6024–6032.
Mansfeld, F., Kending, M.W., Tsai, S., 1982. Corrosion 38, 570.
Morad, M.S., Kamal El-Dean, A.M., 2006. Corros. Sci. 48, 3398.
Moretti, G., Quartarone, G., Tassan, A., Zingales, A., 1996. Electrochem. Acta 41, 1971.
Basics of corrosion measurements, Application note no. 1, (EG&G PRINSTON APPLIED RESEARCH): (1982) pp. 1.
Putilova, I.N., Balezin, S.A., Barannik, V.P., 1960. Metallic Corrosion Inhibitors. Pergamon Press, NY, pp. 14.
Quraishi, M.A., Rawat, J., 2002. Mater. Chem. Phys. 73, 118–122.
Ross Macdonald, J., 1987. Impedance Spectroscopy. John Wiley and Sons.
Sieverts, A., Lueg, P., 1923. Z. Anorg. Chem. 126, 192.
Tsuru, T., Haruyama, S., Boshoku Gijutsu, B., 1978. J. Jpn. Soc. Corros. Eng. 27.
Zhang, Q.B., Hua, Y.X., 2009. Electrochim. Acta 54, 1881–1887.